Society of Petroleum Engineers

SPE-191778-18ERM-MS

Contribution of Hydraulic Fracture Stage on the Gas Recovery from the Marcellus Shale

Mohamed El sgher, Kashy Aminian, and Samuel Ameri, West Virginia University

This paper was prepared for presentation at the SPE Eastern Regional Meeting held in Pittsburgh, Pennsylvania, USA, 7 - 11 October 2018.

Abstract

The natural gas from Marcellus Shale can be produced most efficiently through horizontal wells stimulated by multi-stage hydraulic fracturing. The objective of this study is to investigate the impact of the geomechanical factors and non-uniform formation properties on the gas recovery for the horizontal wells with multiple hydraulic fractures completed in Marcellus Shale.

Various information including core analysis, well log interpretations, completion records, stimulation design and field information, and production data from the Marcellus Shale wells in Morgantown, WV at the Marcellus Shale Energy and Environment Laboratory (MSEEL) were collected, compiled, and analyzed. The collected shale petrophysical properties included laboratory measurements that provided the impact of stress on core plug permeability and porosity. The petrophysical data were analyzed to estimate the fissure closure stress. The hydraulic fracture properties (half-length and conductivity) were estimated by analyzing the completion data with the aid of a commercial P3D fracture model. In addition, the information from the published studies on Marcellus Shale cores plugs were utilized to determine the impact of stress on the propped fracture conductivity and fissure permeability. The results of the data collection and analysis were utilized to generate a base reservoir model. Various gas storage mechanisms inherent in shales, i.e., free gas (matrix and fissure porosity), and adsorbed gas were incorporated in the model. Furthermore, the geomechanical effects for matrix permeability, fissure permeability, and hydraulic fracture conductivity were included in the model. A commercial reservoir simulator was then employed to predict the gas production for a horizontal well with multi-stage fracture stimulation using the base model. The production data from two horizontal wells (MIP-4H and MIP-6H), that were drilled in 2011 at the site, were utilized for comparison with the model predictions. The model was then also used to perform a number of parametric studies to investigate the impact of the geomechanical factors and non-uniform formation properties on hydraulic fractures and the gas recovery.

The matrix permeability geomechanical effect was determined by an innovative method using the core plug analysis results. The results of the modeling study revealed that the fracture stage contribution has a more significant impact on gas recovery than the fracture half-length. Furthermore, the predicted production by the model was significantly higher than the observed field production when the geomechanical effects were excluded from the model. The inclusion of the geomechanical factors, even though it reduced the

differences between the predictions and field results to a large degree, was sufficient to obtain an agreement with field data. This lead to the conclusion that various fracture stages do not have the same contribution to the total production. Based on well trajectory, variation in instantaneous shut-in pressure ISIP along the horizontal length, shale lithofacies variation and natural fracture (fissure) in the reservoir, it is possible to estimate the contribution of different stages to the production for both wells MIP-4H and MIP-6H.

Introduction

The Marcellus Shale play is estimated to contain over 140 trillion cubic feet of recoverable natural gas. The Marcellus play has developed into the largest natural gas play in the United States. Furthermore, the Marcellus Shale is one of the largest unconventional gas shale plays in the United States. It underlies much of West Virginia, Pennsylvania, and New York state, and extends under Lake Erie and into Canada. Additionally, the energy demand is increasing dramatically in the United States and internationally. The production of natural gas is gaining importance since it is considered to be a cleaner source of energy compared to other sources. There are much natural gas plays across the United States, with the Marcellus Shale play being the largest resource. The Marcellus Shale plays a vital role in the future of gas production and encompasses several states in the eastern United States.

Hydraulic fracture propagation in the naturally fractured reservoir is significantly different from hydraulic fracture propagation in non-fractured reservoirs. In naturally fractured reservoirs, the fracture may propagate asymmetrically due to hydraulic fracture interaction with the natural fractures. However, hydraulic fracture propagates symmetrically perpendicular to the minimum stress in non-fractured reservoirs because rock properties are homogenous. Furthermore, natural fracture and hydraulic interaction may cause substantial diversion of hydraulic fracture paths due to the intersection with natural fractures, which causes difficulties in proppant transport and, finally, job failure.

This paper investigates the contribution of different stages to the total production for both of the wells (MIP-4H and MIP-6H). Using analysis based on well trajectory, variation in ISIP along the horizontal length, shale lithofacies variation and natural fracture (fissure) in the reservoir, it is possible to know which stage contributes to the total production.

Background

Shale gas reservoirs have become a growing source of natural gas reserves across the United States. The use of horizontal drilling and hydraulic fracturing are key aspects of successfully developing this important natural gas resource. A horizontal well with multiple hydraulic fractures improves the contact area and creates a conductive pathway for the flow of hydrocarbon into the wellbore (Boosari, Eshkalak, and Aybar 2015). This technique significantly improves hydrocarbon recovery in shale reservoirs. The horizontal wells are completed in stages, and each stage is fractured. Diagnostic data in the field, however, has shown that in most cases not all stages create dominant fractures (Fisher et al. 2004; Molenaar et al. 2011). Many studies have investigated production variability from the horizontal length. Miller et al. (2011) and Slocombe et al. (2013) analyzed production logs for over 100 horizontal shale-gas wells and concluded that there is production variability along the horizontal length and only about 64% of perforation clusters contributed to the total production. Cipolla et al. (2011) applied a statistical analysis on 100 production logs from geometrically completed horizontal wells, and their results indicated that only 60% of perforation clusters contribute to production. Chorn et al. (2014) studied production performance for 100 wells drilled in the Barnett Shale and observed significant production variability. Also, Spain et al. (2015) discovered that 40-60% of perforation clusters are either producing minimum amounts of gas or not producing at all. Ugueto et al. (2016) found that only 50-60% of the perforation clusters were properly stimulated or produced at significant rates based on the fiber optic diagnostics.

Lateral heterogeneity of the reservoir properties (reservoir mineralogy, rock quality, and facies change over a short distance) has an impact on the fracture propagation. Furthermore, natural fractures (fissure) distribution within shale have significant effects on horizontal stimulation. Many researchers have observed that significant variation in reservoir properties is present along the lateral interval. This variation could affect the initiation and propagation of hydraulic fractures, as well as the productivity of the well. Researchers observed the variation by using image logs, sonic logs, and microseismic data along the horizontal wellbore. Hydraulic fractures propagate in the path of least resistance; consequently, it is essential to isolate high-stress zones from low-stress zones, as well as naturally fractured zones from un-fractured zones to maximize stimulation effectiveness (Baihly et al., 2010; Wutherich et al. 2012). Furthermore, Figure 1 illustrates hundreds of fracture stages which are disturbed from left to right, showcasing deepest to shallowest. It is noticeable that the hydraulic fracture extends upward rather than downward because the Onondaga Limestone below the Marcellus Shale acts as fracture barriers (Fisher et al. 2010). Serajian and Ghassemi (2011) and Suarez-Rivera et al. (2011) revealed that shale intervals, which have low clay content, have proven easier to hydraulically fracture, both during drilling and during stimulation. This is based on borehole image data and fracture initiation pressures encountered during stimulation. Furthermore, Waters et al. (2006) observed that clay-rich intervals are likely to show higher horizontal stresses. Therefore, hydraulic fracture initiation and proppant placement become more difficult in these zones.

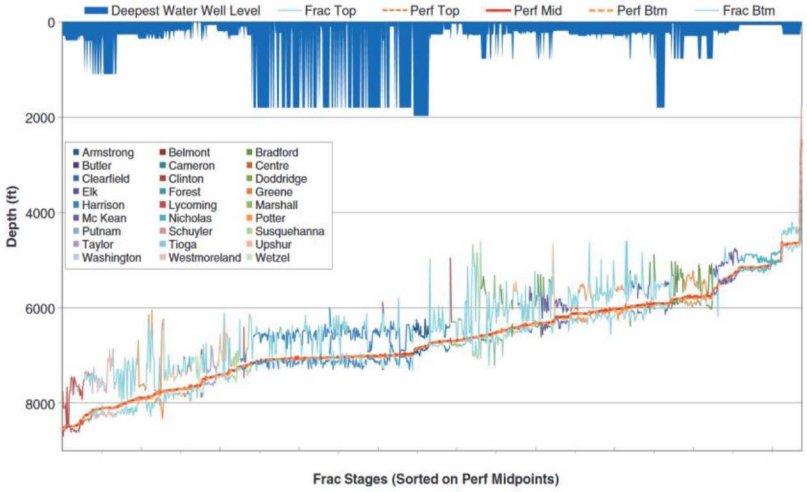

Figure 1—Illustrates the Vertical Extension of the Hydraulic Fracture in Marcellus Shale (Fisher et al. 2010)

Reservoir Geomechanics

When gas is produced from the reservoir, net stress increases due to the decrease in pore (gas) pressure, while the overburden pressure remains constant. This results in a reduction in the size of pores in the matrix and fissure, as well as the proppant embedment in the propped fracture. Many researchers have been incorporated impact of stress dependent permeability (matrix, fissure and Hydraulic fracture) in reservoir modeling (El Sgher et al. 2018; and Sina Hosseini Boosari, Aybar, and Eshkalak 2016)

Naturally fractured reservoirs are characterized by matrix and fractures systems and tend to be more sensitive to stress variations than non-fractured formations (Lian et al., 2012). Dong et al. (2010) measured the stress-dependent matrix permeability of fine-grained silty-shale. They suggested that the dependency of gas permeability to stress can be better expressed using a power law function. Additionally, Shi and Durucan (2016) measured matrix permeability as a function of net pressure. Heller et al. (2014) measured shale matrix permeability as a function of net pressure by using helium under various pore pressures. The six core samples analyzed in Heller et al.'s study were from the Barnett, Marcellus, Eagle Ford, and Montney

formations. Most of the studies mentioned above, including Dong et al. (2010), Shi and Durucan (2016) and Heller et al. (2014), considered the entire range of the data representing matrix permeability.

Elsaig et al. (2017) measured the absolute permeability of Marcellus Shale core plugs at four different gas pressures and seven different net stress values. The absolute permeability was determined at each net stress level by the application of the double slippage correction. Figure 2 shows the impact of net stress on the absolute permeability determined during these experiments. Fissures that are more sensitive to stress close down as stress increases. The closure of fissures causes a major reduction in the measured permeability of the core plug. After all the fractures close, the permeability reduction is related only to the matrix compression. Walsh (1981) suggested that when $(k/k_o)^{1/3}$, where k is the permeability measured at a specific stress (P), and k_o is the permeability measured at the lowest stress (P_o) values, is plotted against ln (P/P_o), a linear trend is observed. Figure 3 illustrates this plot for the above-mentioned Marcellus Shale core plug (Elsaig et al. 2016). The difference in the compressibility of the fissures and the matrix resulted in two straight lines on this plot. The net stress value at which these two lines intersect represents the point that fissures are closed (closure stress).

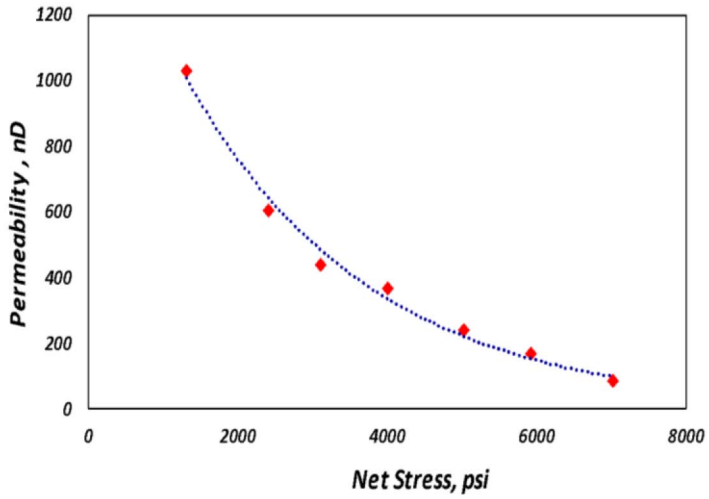

Figure 2—The Impact of net stress on the Absolute Permeability (after SPE 184042)

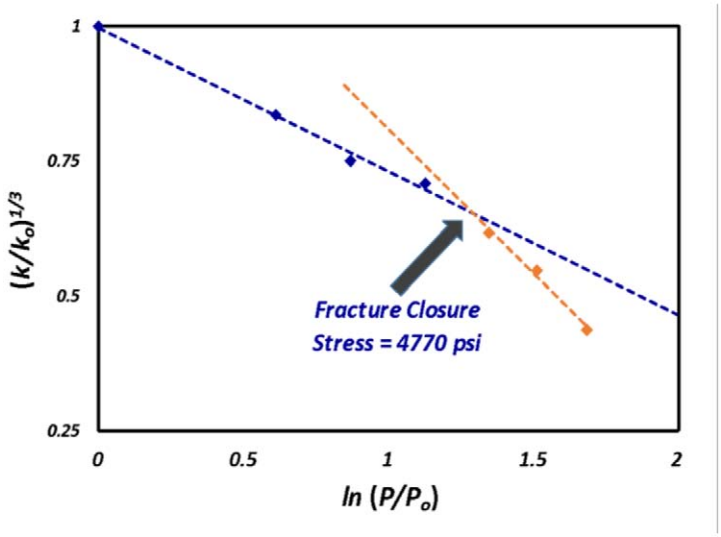

Figure 3—Evaluation of Fissure Closure Stress (after SPE 184042)

Laboratory data published by Fredd et al. (2001) illustrates the impact of the stress on un-propped and partially propped fracture conductivity for a formation with high Young's modulus. Cipolla et al. (2008) extrapolated Fredd et al.'s data to lower Young's modulus as illustrated in Figure 4.

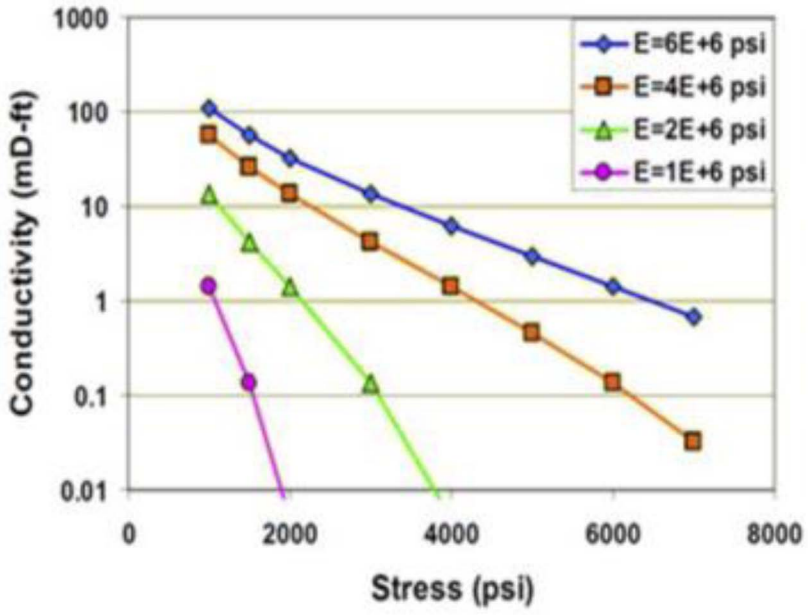

Figure 4—Effect of Young's Modulus and Net Stress on Conductivity of Un-Propped Fractures (After Cipolla et al. 2008)

McGinley et al. (2015) conducted a number of experiments to measure the conductivity of the propped hydraulic fractures in the Marcellus Shale as a function of the net stress. The core plugs used in their study were collected at two different locations: Elimsport and Allenwood. The core plugs were cut perpendicular and parallel to the bedding planes in order to investigate the effect of anisotropy on fracture conductivity. Figures 5 and 6 illustrate the results of these experiments for the Elimsport and Allenwood samples.

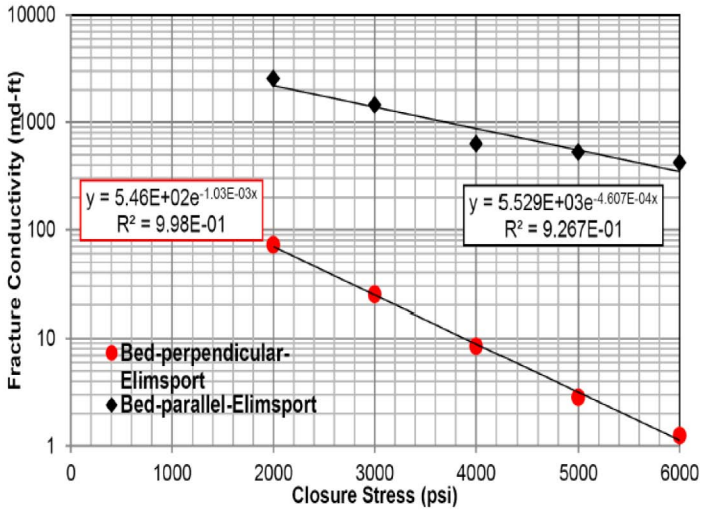

Figure 5—Measured Propped Fracture Conductivity versus Closure Stress for Elimsport Samples (McGinley et al., 2015)

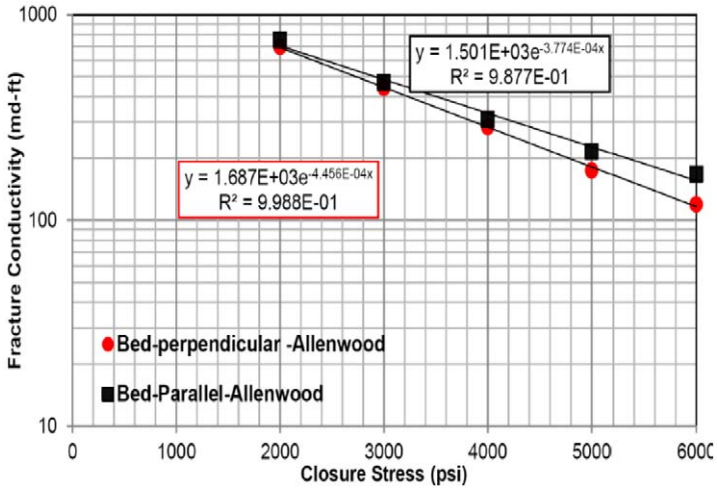

Figure 6—Measured Propped Fracture Conductivity versus Closure Stress for Allenwood Samples (McGinley et al., 2015)

Objective and Methodology

The objective of this study was to investigate the impact of the geomechanical factors and non-uniform formation properties on the gas recovery for the horizontal wells with multiple hydraulic fractures completed in Marcellus Shale. In this study, numerical reservoir simulation techniques were used to predict production performance of the horizontal wells with multiple hydraulic fractures completed in Marcellus Shale. In order to accomplish the objective of this study, a methodology consisting of the following steps were implemented:

Data Collection

The data used in this study was acquired from the Marcellus Shale Energy and Environment Laboratory (MSEEL), which is located in the Morgantown Industrial Park (MIP) site in the state of West Virginia. MSEEL is a field laboratory operated by Northeast Natural Energy (NNE). This site includes two horizontal wells (MIP-4H and MIP-6H) that were drilled in 2011. Moreover, two horizontal wells (MIP-3H and MIP-5H) and a vertical science observation well (MIP-SW) were drilled in 2015. The science well provided an opportunity for collecting subsurface samples and microseismic monitoring.

1. The results of the core analysis performed through the Precision Petrophysical Analysis Laboratory (Elsaig et al. 2016) discussed earlier were used in this study.
2. The geomechanical rock properties including the minimum horizontal stress, Young's modulus, and Poisson's ratio were estimated from the logs.
3. Completion and production data for two horizontal wells, MIP-4H and MIP-6H, were obtained from the MSEEL project. Well MIP-4H was stimulated with eleven fractures over a lateral of 3800 ft. Well MIP-6H was stimulated with eight fracture stages over a lateral length of 2,380 ft. The production records included 1473 days of production for both wells.
4. The fracture treatment for both wells, MIP-4H and MIP-6H, used a pump rate of 80 bpm. 339,172 gallons of a slick water; 1500 gallons of acid; 36,175 gallons linear 2000; and 400,000 lb of sand which included 100,000 lb of 100 lb of mesh and 300,000 lb of 40/100 mesh were used in each stage. The hydraulic fracture properties were estimated from the completion data by employing a P3D fracture modeling software (FRACPRO) which assumes isotropic rock properties for estimating the fracture properties.
5. Information on the magnitude of minimum horizontal stress (Sh_{min}) for both wells MIP-4H and MIP-6H at a given depth are available from the pumping records for each fracture stage, which is instantaneous shut-in pressure (ISIP). Figures 7 and 8 show the variation of instantaneous shut-in pressure (ISIP) along the well as well as Gamma Ray log readings.

6. Figures 9 and 10 show a variation of Gamma Ray along the horizontal section of both wells MIP-4H and MIP-6H with well trajectory in the vertical direction. The thickness of the pay zone of the Marcellus shale is around 90 feet, starting from 7460 ft. to 7555 ft., as it seen in Figure 11.
7. Marcellus interval is composed of six shale lithofacies based on the mineralogy and organic content (Paronish et al., 2016) as it can be seen in Figure 11 for both wells MIP-3H and MIP-4H. The sex different facies units are Organic Siliceous Shale, Organic Mudstone, Organic Mixed Shale, Gray Siliceous Shale, Gray Mixed Shale and Gray Mudstone. Furthermore, mineralogy controls the brittleness in Shale lithofacies. Gray Mudstone and Organic Mudstone facies are more ductile due to an increase in clay content, and Gray Siliceous and Organic siliceous shale are more brittle due to an increase in quartz content. Lateral variation in facies is notable between the two wells based on lateral mineralogy changes.

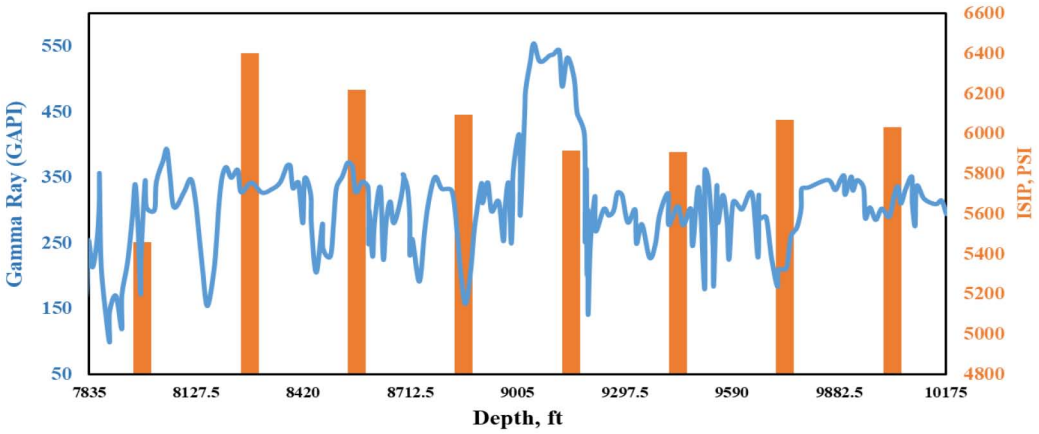

Figure 7—Instantaneous Shut-in Pressure (ISIP) per Stage for Well MIP-6H

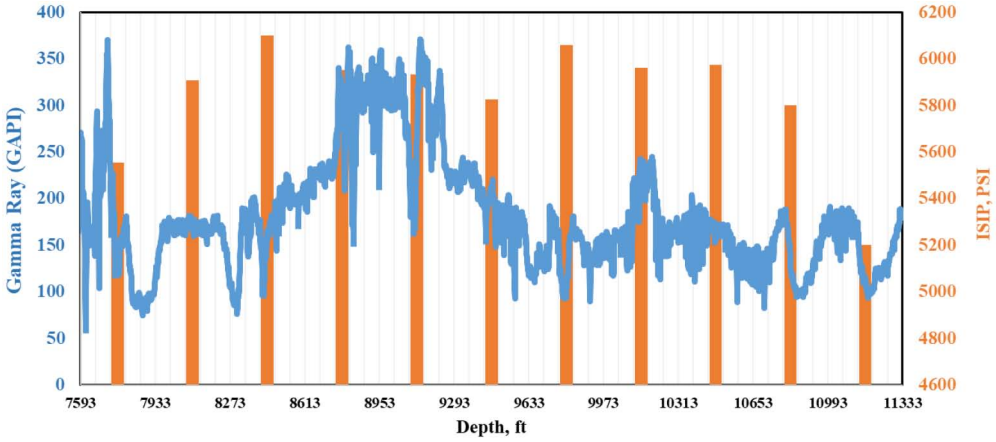

Figure 8—Instantaneous shut-in pressure (ISIP) per stage for well MIP-4H

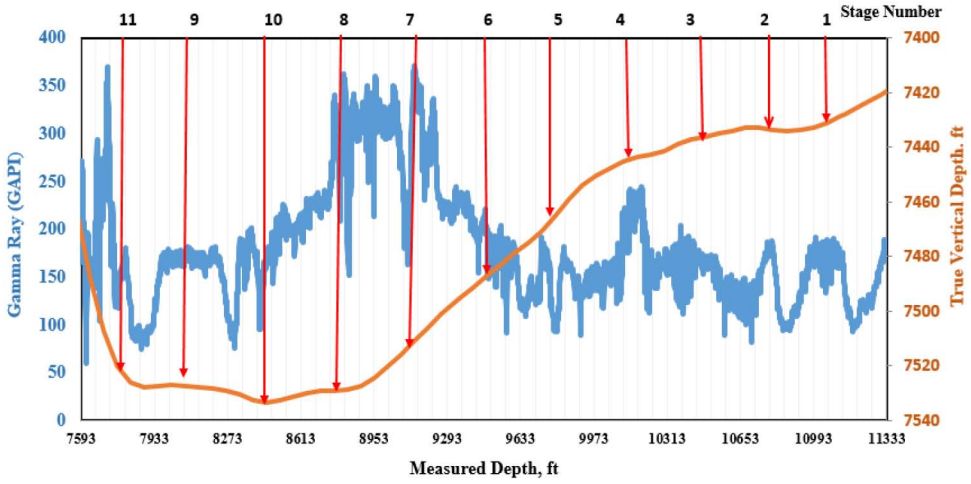

Figure 9—Well Trajectory with a Variation of Gamma Ray along the Horizontal Section of MIP-4H

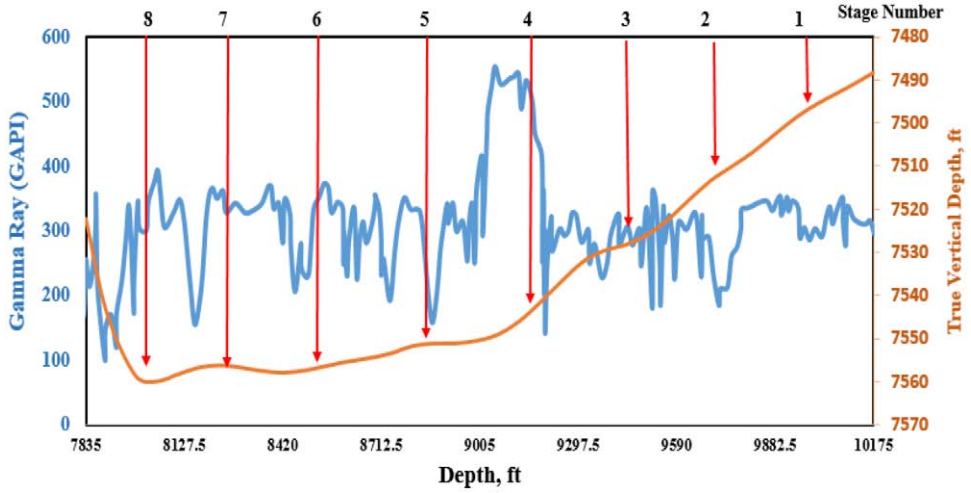

Figure 10—Well Trajectory with a Variation of Gamma Ray along the Horizontal Section of MIP-6H

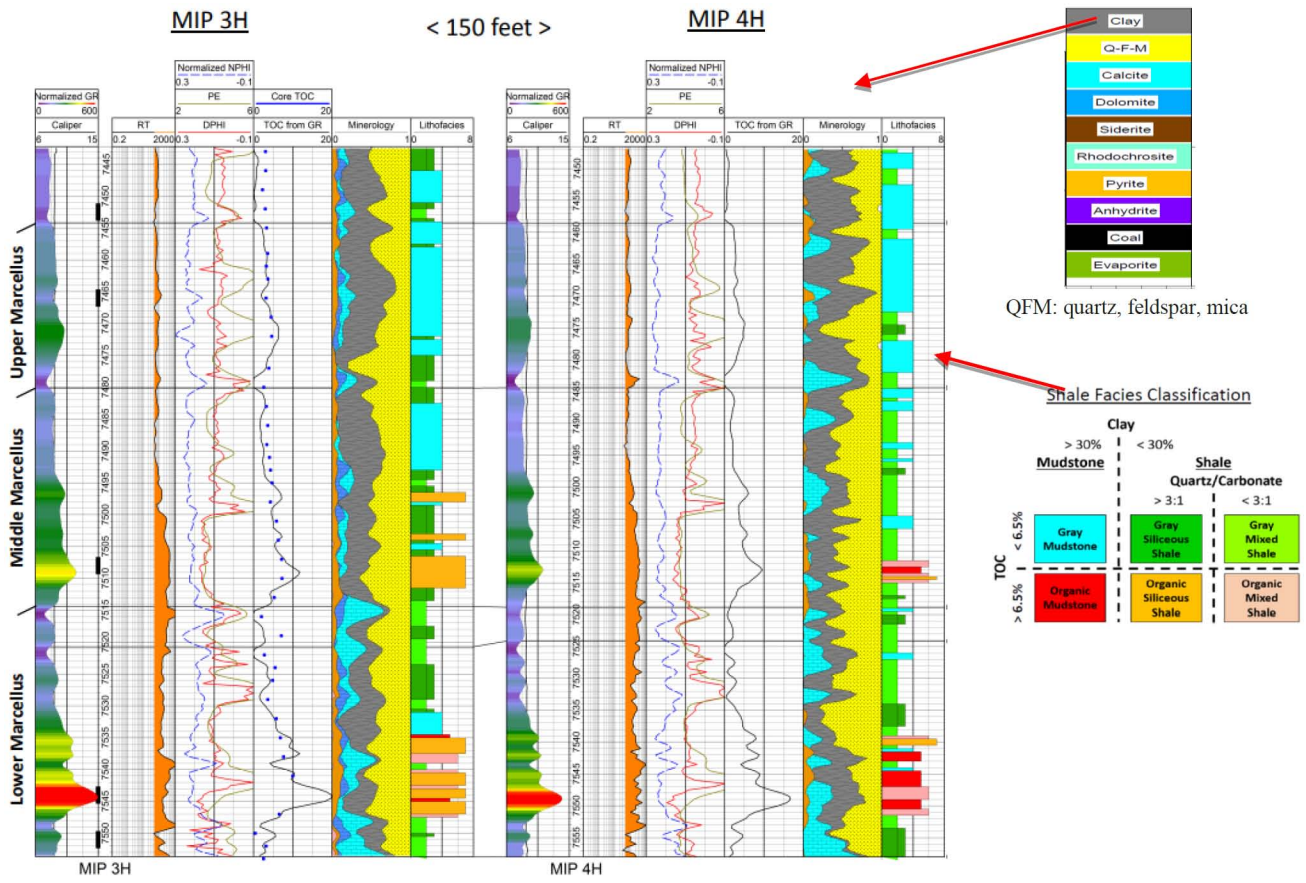

Figure 11—GR, RT, TOC FROM GR and Core, Mineralogy and Lithofacies for 3H & 4Hwells (Paronish et al., 2016)

Model Development

A reservoir simulation model (CMG-GEM, 2016) was used to develop the base models for wells MIP-4H and MIP-6H. A Logarithmically Spaced, Locally Refined, Dual-Permeability (LS-LR-DK) reservoir model was adopted to effectively simulate the complex hydraulic fracture and natural fracture behavior. The dual permeability model was selected to incorporate the naturally fractured nature of shales, and the logarithmic refinement was required to capture the transient effects around the hydraulic fracture. Evenly spaced gridding would allow for the fine gridding required around the fracture, but it would create unnecessary grid refinement far away from the fracture. In the dual-permeability model, flow can occur from fracture to fracture, matrix to matrix, and matrix to fracture. The values of the Langmuir Pressure and Volume for Marcellus Shale measured by Zamirian et al. (2015) were incorporated in the base models. In the CMG model, the fissure permeability for the dual-permeability was defined using Equation 1 below to represent the flow from one fracture block to another (GEM, 2016)

$$\text{Fissure Permeability} = \frac{\text{Fissure Conductivity}}{\text{Fissure Spacing}} \tag{1}$$

The natural fracture conductivity was assumed to be 0.02 md-ft following the work by El Sgher et al. (2018). Relative permeability curves for flow in the shale matrix were generated using the Corey Model. Curves for water-oil relative permeability and liquid-gas relative permeability are presented in Figures 12 and 13. For natural fractures and hydraulic fracture, relative permeability curves were assumed straight-line in many reservoir simulators. The values of relative permeability changed linearly from 0 to 1. Oil-water relative permeability remained unchanged since no oil was produced while the liquid-gas was allowed to change as stress changed for the matrix, natural fracture, and hydraulic fracture.

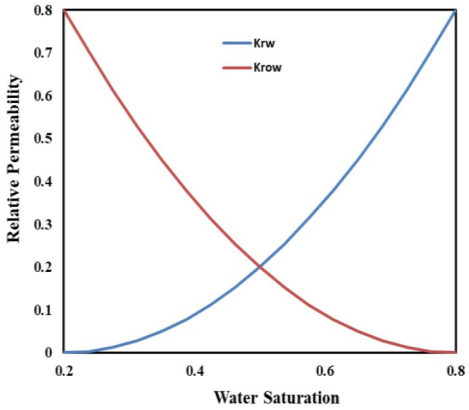

Figure 12—Relative Permeability Curve for the Water Phase

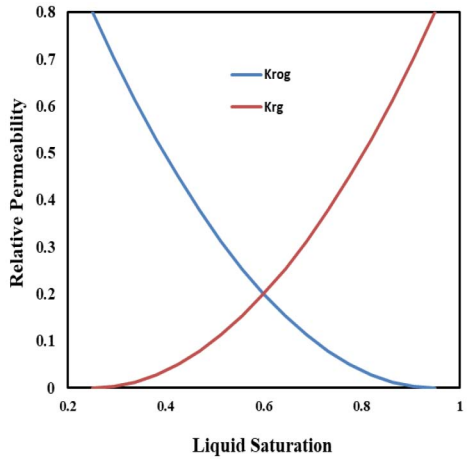

Figure 13—Relative permeability Curve for the Gas Phase

Additionally, wellbore pressures for wells MIP-6H and MIP-4H were calculated from tubing pressure and used as constraints in the simulation model for history matching. Figures 14 and 15 show wellbore pressures for wells MIP-6H and MIP-4H.

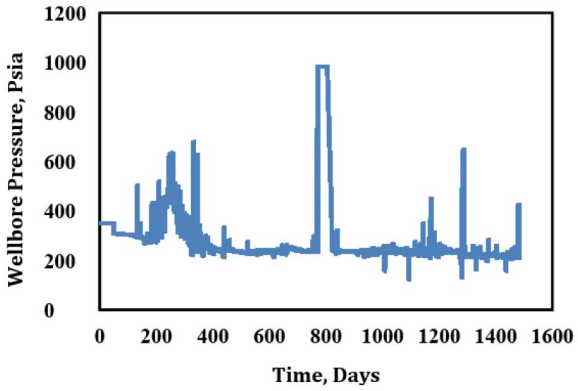

Figure 14—Wellbore pressure for well MIP-6H

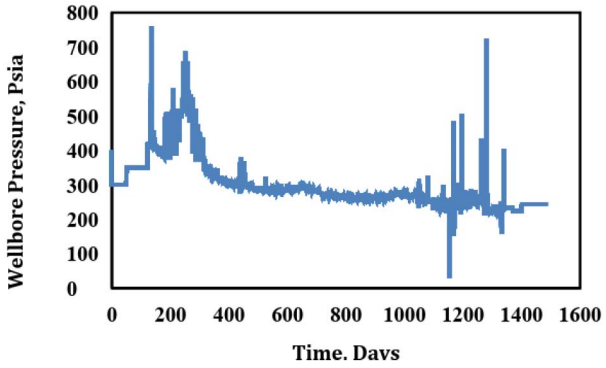

Figure 15—Wellbore pressure for well MIP-6H

The results of data collection and analysis were used as inputs to develop the base models for wells MIP-6H, and MIP-4H are summarized in Table 1.

Table 1—Basic Model Parameters for MIP-4H and 6H

Reservoir Parameters	Value	Unit
Model dimensions (MIP-6H)	4000 Length× 1500 Width × 90 Height	ft.
Model dimensions (MIP-4H)	4500 Length× 1500 Width× 90 Height	ft
Initial Reservoir Pressure	4700	psia.
Fissure Porosity	0.0001	Fraction
Matrix Porosity	0.045	Fraction
Initial Fissure Permeability i, j, k	0.001,0.001,0.0001	md
Initial Matrix Permeability i, j, k	0.00045,0.00045,0.000045	md
Gas Saturation	0.85	Fraction
Water Saturation	0.15	Fraction
Initial Water Saturation $_{HF}$	0.6	Fraction
Initial Water Saturation connected with hydraulic fracture $_{NF}$	0.6	Fraction
Initial Water Saturation not connected with hydraulic fracture $_{NF}$	0.1	Fraction
Density	120	lb/ft^3
Langmuir Pressure	500	psi
Langmuir Volume	0.12	gmol/lb
Fraction Spacing for (MIP-6H)	340	ft.
Fraction Spacing for (MIP-4H)	380	ft.
Initial Horizontal Fracture Conductivity	15	mD-ft.
Initial Vertical Fracture Conductivity	1500	

To incorporate the stress-dependent matrix permeability in the model, the permeability measurements illustrated in Figure 2 were utilized. As discussed earlier, the permeability values at stress values higher than the closure pressure represent only the matrix permeability. These permeability values were utilized to develop the relation between matrix permeability and the net stress using a logarithmic equation, following the work by El Sgher et al. (2018). To incorporate the stress-dependent fissure permeability in the model, the curve for Young's modulus of 2E+6 psi in Figure 4 was used. Young's modulus of 2E+6 psi was used in

this study because Marcellus Shale is a relatively soft formation (Stegent et al. 2010). The initial net stress in the formation was estimated to be 2600 psi and the maximum net stress was estimated to be 6800 psi. The matrix and fissure permeability values between 2600 psi and 6800 psi were then normalized and converted to permeability multipliers as a function of the reservoir pressure (pore pressure). The matrix and fissure permeability multipliers that were used in the reservoir model are provided in Figure 16. This is the same procedure that was employed by El sgher et al. (2018)

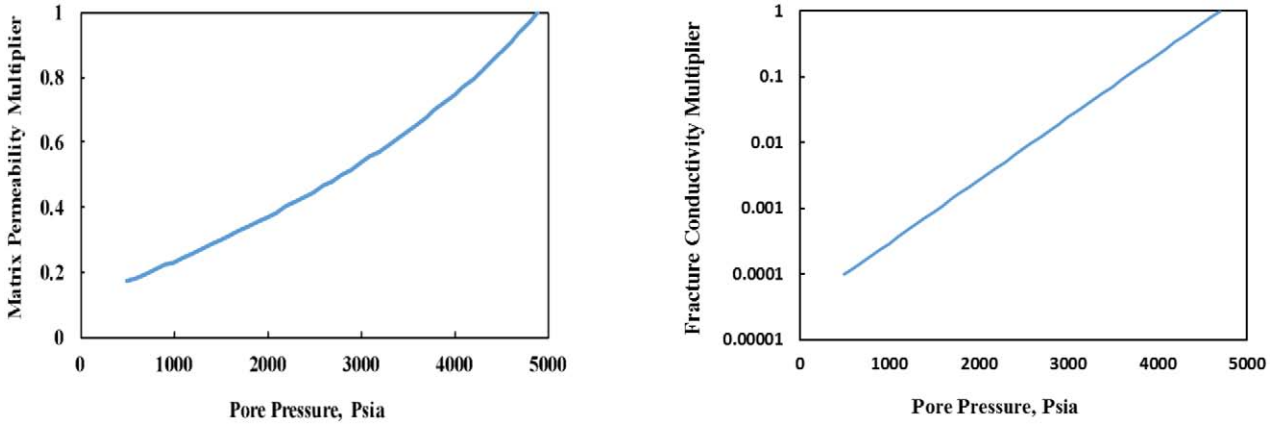

Figure 16—Matrix and Fissure Permeability Multiplies

To incorporate stress-dependent propped fracture conductivity into the model, only the results from the Elimsport sample were utilized, shown in Figure 5. This is because the stress and anisotropy impacts were more pronounced in this case (El sgher et al. 2018). The conductivity values at 2600 psi in Figure 5 were considered to be the initial conductivity of propped fracture. Propped fracture conductivity multipliers were obtained based on the same method used for matrix and fissure permeability multipliers. Figures 17 illustrates propped fracture conductivity multipliers.

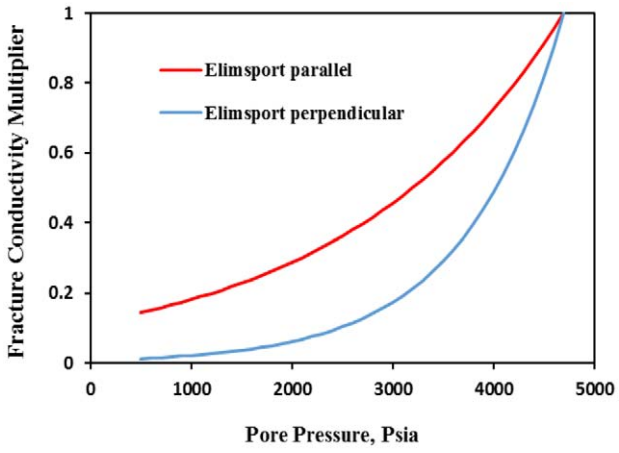

Figure 17—Fracture Conductivity Multiplier for Elimsport Sample

Contribution of Hydraulic Fracture Stage to Total Production

To investigate the contribution of hydraulic fracture stage to total production, production data for MIP-4H and MIP-6H were used for history matching. Four different cases were modeled for each horizontal well to achieve a match. These cases are as follows:

1. Non-fractured reservoir, all hydraulic fractures were assumed to have the same length, and other properties included geomechanical (matrix and hydraulic fracture).

2. Naturally fractured reservoir, all hydraulic fractures were assumed to have the same length, and other properties included geomechanical (matrix, fissure and hydraulic fracture). Furthermore, uniform fissure distribution was considered along the horizontal well length with 20-ft horizontal spacing (El sgher et al. 2017).
3. One stage was assumed to be non-productive based on well trajectory and variation in instantaneous shut-in pressure (ISIP) along the horizontal well length.
4. Two stages were assumed to be non-productive based on well trajectory and variation in instantaneous shut-in pressure (ISIP) along the horizontal well length.

History matching for water production was performed for both wells. Relative permeability curves were assumed straight-line for natural fracture and hydraulic fracture. Before the history matching, initial water saturation in the hydraulic fracture was assumed to be 100%, initial water saturation in the natural fracture was about 100% near the hydraulic fracture, and to be 10% far away from a hydraulic fracture. After these assumptions were made, the model produced more water than the production data. To achieve the history match, the endpoint of the relative permeability was reduced to change the shape of the relative permeability curves. Furthermore, initial water saturation for hydraulic fracture and natural fracture were changed during history matching.

Result and Discussion

The results of the fracture-modeling software are provided in Table 2 and 3 for MIP-4H and MIP-6H. It should be noted that even with good quality input data, the fracture properties in shale cannot be accurately estimated because of complex interactions of rock, stress, and natural fracture characteristics. Furthermore, the large fracture height growth was suspected because of low in-situ stress contrast between the pay zone and its adjacent zones for both wells MIP-4H and MIP-6H. Fracture barriers are necessary in the stratigraphic section to control the fracture height. Consequently, the stimulation energy is conducted away from the shale, which reduces the efficiency of well stimulation and causes the induced fractures to intersect any nearby water-bearing zone. As it can be seen in Figures 7, 8, 9, and 10, some sections of both horizontal wells are out of the pay zone, and there is variation in ISIP along the horizontal length for both wells. Therefore, it is very likely that some of the stages are non-contributing. Furthermore, Gray Mudstone and Organic Mudstone facies are more ductile due to higher clay content. As it is seen in Figure 11, Gray Mudstone is more abundant at the top of the pay zone, and Organic Mudstone is more abundant at the bottom of the pay zone for MIP-4H.

Table 2—Hydraulic Fracture Properties for MIP-6H

Treat #	Top Depth MD	Bottom Depth MD	Fracture Half-Length	Height	Average Fracture Width	Average Conductivity
	(ft)	(ft)	(ft)	(ft)	(ft)	(mD·ft)
1	9935	10175	500	377	0.07	179
2	9635	9875	491	379	0.07	175
3	9335	9575	483	377	0.07	171
4	9035	9300	468	380	0.07	162
5	8735	8975	455	384	0.07	148
6	8435	8675	450	386	0.08	148
7	8135	8375	448	386	0.08	147
8	7835	8075	468	380	0.07	157

Table 3—Hydraulic Fracture Properties for MIP-4H

Treat #	Top Depth MD	Bottom Depth MD	Fracture Half-Length	Height	Average Fracture Width	Average Conductivity
	(ft)	(ft)	(ft)	(ft)	(ft)	(mD·ft)
1	11093	11333	559	417	0.05	153
2	10743	11023	566	414	0.05	157
3	10393	10708	568	414	0.05	158
4	10043	10323	574	412	0.05	159
5	9693	9973	695	366	0.04	153
6	9343	9623	708	366	0.04	152
7	8993	9273	700	367	0.04	148
8	8643	8923	692	365	0.04	144
9	8293	8573	688	365	0.05	142
10	7943	8223	691	365	0.05	146
11	7593	7873	710	368	0.04	145

For Case 1, non-fractured reservoir, the history match was obtained by adjusting the fracture half-length. The fracture half-length and fracture conductivity predicted for both of the wells (MIP-4H and MIP-6H) by P3D fracture model matches fracture half-length and fracture conductivity obtained from reservoir simulation. The values of the hydraulic fracture half-length acquired from history matching for case 1 for both wells are provided in Tables 4. Figure 18 show Production history matching for Wells MIP-6H & MIP-4H.

Table 4—Hydraulic Fracture Half-length for MIP-6H & MIP-4H

MIP-6H		
Stage Number	Fracture Half-Length (ft)	Average Conductivity (mD-ft)
1	500	179
2	491	175
3	483	171
4	468	162
5	455	148
6	450	148
7	448	147
8	468	157

MIP-4H		
Stage Number	Fracture Half-Length (ft)	Average Conductivity (mD-ft)
1	559	153
2	566	157
3	568	158
4	574	159
5	695	153
6	708	152
7	700	148
8	692	144
9	688	142
10	691	146
11	710	145

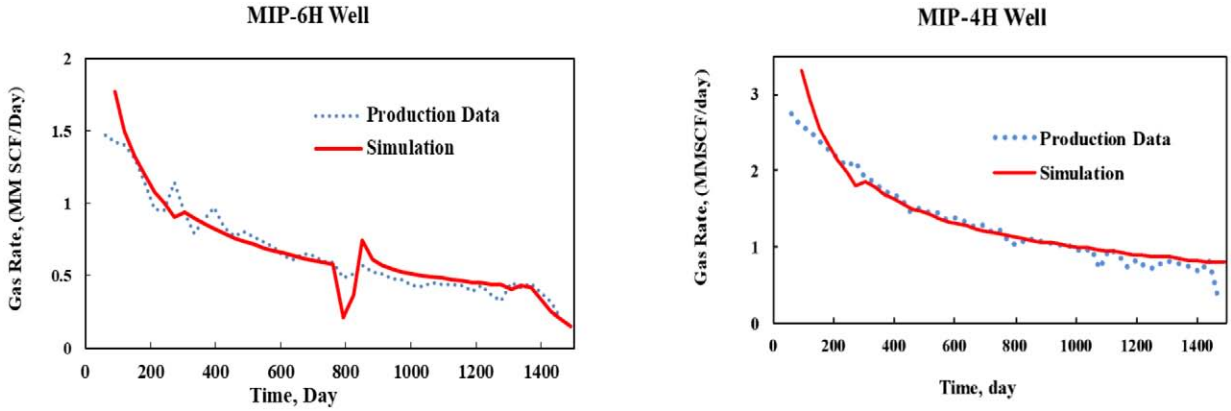

Figure 18—Production History matching for Wells MIP-6H & MIP-4H

Case 2, naturally fractured reservoirs, the history match was obtained by adjusting the fracture half-length. The fracture half-length and fracture conductivity predicted for both of the wells (MIP-4H and MIP-6H) by P3D fracture model resulted in significantly higher production than observed from the field data. Figure 19 illustrates the match between the simulation results and the actual field production data from well MIP-4H and MIP-6H for 1473 days. Fracture half-lengths predicted from P3D model are higher than those predicted by the production history matching for a naturally-fractured reservoir.

Figure 20 illustrates the final match between the simulation results and the field water flow rates for MIP-4H and MIP-6H wells. History matching was achieved by reducing initial water saturation from 100% to 60% for hydraulic fracture and natural fracture. Additionally, the endpoint of the relative permeability to water was reduced from 1 to 0.8 for hydraulic fracture and natural fracture.

Table 5—Hydraulic Fracture Half-length for MIP-6H & MIP-4H

Well	MIP-6H	MIP-6H
Fracture Half-Length, X_f ft	420	620

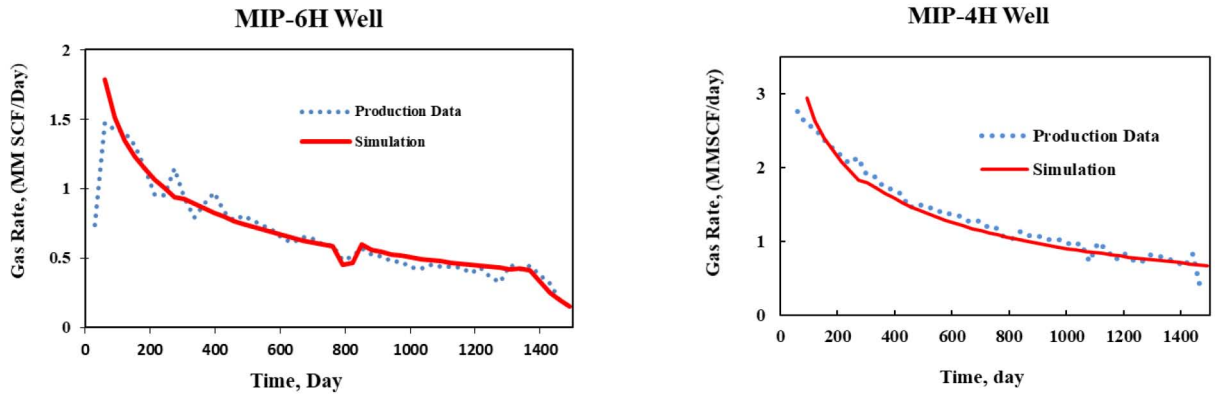

Figure 19—Production History matching for Wells MIP-6H & MIP-4H

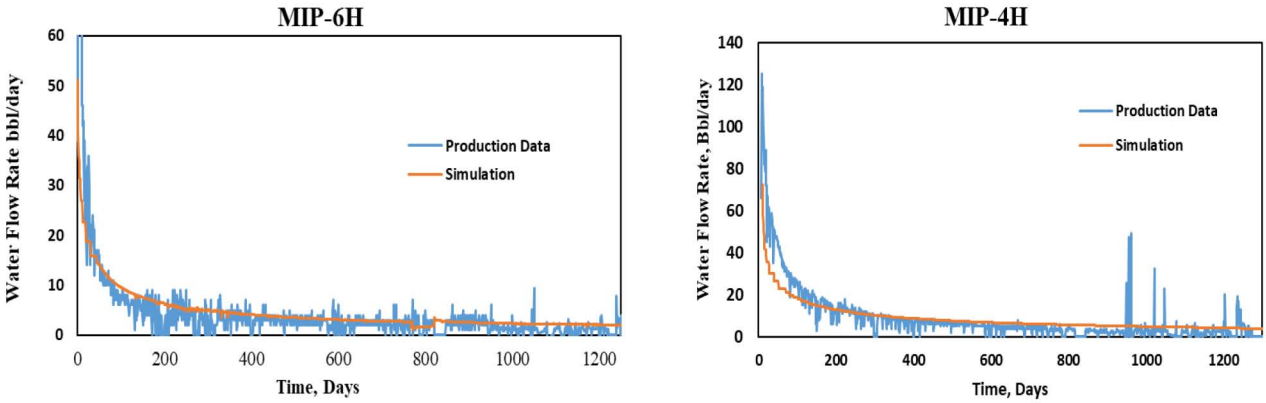

Figure 20—Production History matching for water rate Wells MIP-6H & MIP-4H

Figure 21 compares the cumulative production, by the model, for well MIP-6H in naturally fractured reservoirs and non-fractured reservoirs. According to Figure 21, non-fractured reservoirs have higher cumulative production than naturally fractured reservoirs.

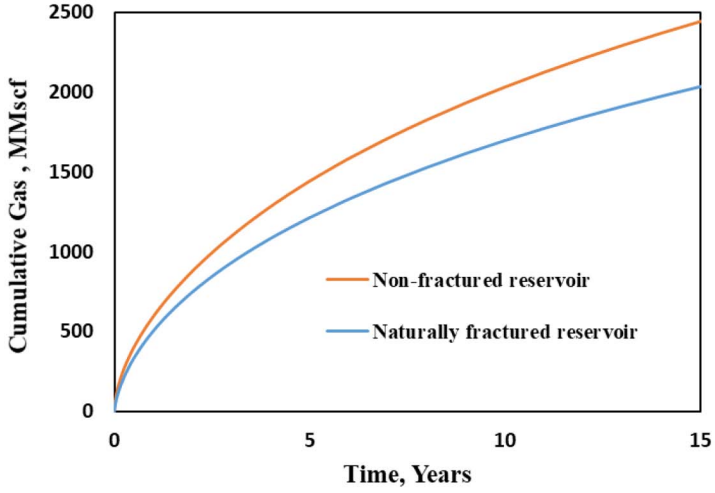

Figure 21—Cumulative gas production for Well MIP-6H in naturally fractured reservoirs and non-fractured reservoir.

For Case 3, one of the fracture stages were assumed to be non-contributing to total production based on well trajectory for both wells as it seen in Figure 22. History matching was achieved by increasing the rest of the stages. The results for the fracture half-length showed in the Table 6.

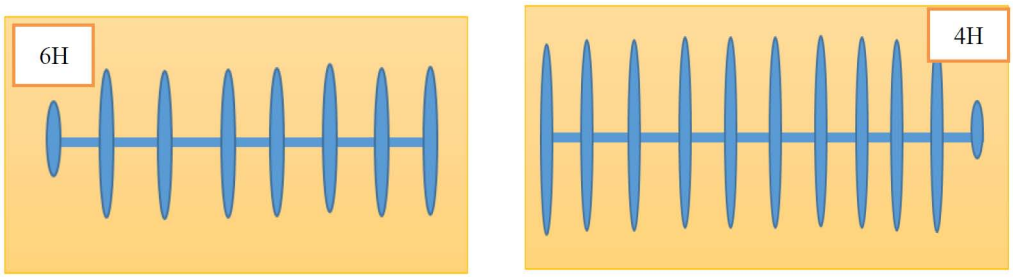

Figure 22—One stages do not contribute to total production for Wells MIP-6H & MIP-4H

Table 6—Hydraulic Fracture Half-length for Wells MIP-6H & MIP-4H

MIP-6H	
Stage Number	Fracture Half-Length (ft)
1	480
2	480
3	480
4	480
5	480
6	480
7	480
8	150

MIP-4H	
Stage Number	Fracture Half-Length (ft)
1	200
2	680
3	680
4	680
5	680
6	680
7	680
8	680
9	680
10	680
11	680

For Case 4, two of the fracture stages were assumed to be non-contributing to total production based on well trajectory for both well as it illustrates in Figure 23. History matching was achieved by increasing the rest of stages. The results for the fracture half-length showed in Table 7.

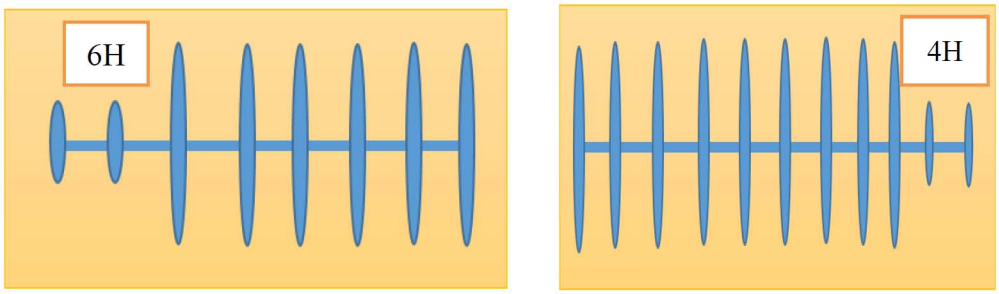

Figure 23—Two stages do not contribute to total production Wells MIP-6H & MIP-4H

Table 7—Hydraulic Fracture Half-length for Wells MIP-6H & MIP-4H

MIP-6H	
Stage Number	Fracture Half-Length (ft)
1	500
2	500
3	500
4	500
5	500
6	500
7	150
8	150

MIP-4H	
Stage Number	Fracture Half-Length (ft)
1	200
2	200
3	700
4	700
5	700
6	700
7	700
8	700
9	700
10	700
11	700

Conclusion

1. Low in-situ stress contrast between the pay zone and its adjacent zones for both well (MIP-4H and MIP-6H) indicated that fracture stimulation was primarily focused above and below the Marcellus Shale, which makes some of the stages non-contributing to total production. Furthermore, MIP-4H and MIP-6H produce water which is entering the shale formation from adjacent stratigraphic due to the height of the fracture out of the pay zone.
2. Variation of instantaneous shut-in pressure (ISIP) along the horizontal well length for both of the wells (MIP-4H and MIP-6H) impacted the hydraulic fracture propagation. The higher instantaneous shut-in pressure (ISIP) and the higher the clay content, it becomes more difficult to propagate the hydraulic fracture. Furthermore, Gray Mudstone and Organic Mudstone facies are more ductile due to higher clay content. Gray Mudstone and Organic Mudstone facies are more abundant at the top and bottom of the pay zone for MIP-4. Therefore, it can be concluded that various fracture stages do not contribute uniformly to total production.
3. Fracture half-length and fracture conductivity predicted for both of the wells (MIP-4H and MIP-6H) by P3D model match fracture half-length and fracture conductivity in the non-fractured reservoir. However, they do not match in the naturally-fractured reservoir.
4. Hydraulic fracturing propagation in the presence of natural fractures will cause the reduction of hydraulic fracture properties (fracture half-length and fracture conductivity) due to the migration of the injection fluid. Therefore, it can be concluded that various fracture stages do not contribute uniformly to the total production.
5. It is essential to determine natural fracture distribution along a horizontal well length which can improve the hydraulic fracture treatment design.

Reference

Baihly, J. D., Altman, R. M., Malpani, R., & Luo, F. (2010, January 1). Shale Gas Production Decline Trend Comparison over Time and Basins. *Society of Petroleum Engineers*.

Boosari, S. Sina Hosseini, Mohammad O. Eshkalak, and Umut Aybar. 2015. "The Effect of Desorption-Induced Porosity-Permeability Changes and Geomechanics on Production from U.S. Shale Gas Formations." 49th U.S. Rock Mechanics/Geomechanics Symposium.

Boosari, S. S. H., Aybar, U., & Eshkalak, M. O. (2016). Unconventional resource's production under desorption-induced effects. *Petroleum*, **2**(2), 148–155.

Cipolla CL Weng X, Mack M, et al. Integrating microseismic mapping and complex fracture model to characterize fracture complexity. In: SPE hydraulic fracturing technology conference, The Woodlands, Texas, USA. 2011.

Cipolla, C.L., Warpinski, N.R., Mayerhofefr, M.J., and Lolon, E.P., and Vincent, M.C.2008. The Relationship between Fracture Complexity, Reservoir Properties, and Fracture Treatment design. Presented at the 2008 SPE Technical Conference and Exhibition. Denver, Colorado, USA, 21-24 September. SPE 115769-MS.

Chorn, L., N. Stegent, and J. Yarus, 2014, Optimizing Lateral Lengths in Horizontal Wells for a Heterogeneous Shale Play: Presented at the SPE/EAGE European Unconventional Resources Conference and Exhibition

Civan, F., 2018a. Effect of stress shock and Pressurization/Depressurization Hysteresis on Petrophysical Properties of Naturally-Fractured Reservoir Formations, paper SPE-190081-MS, the SPE Western Regional Meeting held in Garden Grove, California, USA, 22-27 April 2018.

Dong, J-J.; Hsu, J-Y.; Wu, W-J.; Shimamoto, T.; Hung, J-H.; Yeh, E-C.; Wu, Y-H.; Sone, H., 2010. of the permeability and porosity of sandstone and TCDP Hole-A, *International Journal of Rock Mechanics and Mining Sciences*, Vol. **47**(7), pp.1141–1157.

Elsaig, M. Aminian, K., Ameri, S., and Zamirian, M. 2016. Accurate Evaluation of Marcellus Shale Petrophysicl Properties.presented at the SPE Eastern Regional Meeting, Canton, Ohio, USA, 13-15 September 2016. SPE-184042-MS.

El sgher, M., Aminian, K., Ameri, S. 2018. The Impact of the Net Stress on Gas Recovery from the Marcellus Shale. SPE Eastern Regional Meeting to be held 7-11 October 2018 in Pittsburgh, PA, USA. SPE-191799-MS.

El sgher, M., Aminian, K., Ameri, S. 2018. Geomechanical Impact on Gas Recovery from Marcellus Shale. Presented at the SPE Western Regional Meeting held in Garden Grove, California, USA, 22-27 April 2018. SPE-190054-MS.

El sgher, M., Aminian, K., Ameri, S. 2018. The Impact of Stress on Propped Fracture Conductivity and Gas Recovery in Marcellus Shale. Presented at the SPE Hydraulic Fracturing Technology Conference held in The Woodlands, TX, USA, 23-25 January. SPE-191799191799-MS.

El sgher, M., Aminian, K., Ameri, S. 2017. The Impact of the Hydraulic Fracture Properties on the Gas Recovery from Marcellus Shale. presented at the 2017 SPE Western Regional Meeting held in Bakersfield, California, USA, 23 April SPE-185628-MS.

Fisher, M., Heinze, J., Harris, C., 2004. Optimizing horizontal completion techniques in the Barnett shale using microseismic fracture mapping. In: SPE Annual Technical Conference and Exhibition.

Fisher, K. and Warpinski, N., *Pinnacle- A Halliburton Service, Hydraulic Fracture-Height Growth: Real Data, Society of Petroleum Engineers Paper, SPE 145949*, 201.

Fredd, C.N., McConnell S.B., Boney C.L. and England K.W. 2001. Experimental Study of Fracture Conductivity for Water-Fracturing and Conventional Fracturing Application. *SPE J.* **6** (3): 288–298. SPE-74138-PA

Heller, R., Vermylen, J., Zoback, M., 2014. Experimental Investigation of Matrix Permeability of Gas Shales, *AAPG Bull.*, **98** (5), 975–995.

Lian, P., & Cheng, L. 2012. The Characteristics of Relative Permeability Curves in Naturally Fractured Carbonate Reservoirs. *Society of Petroleum Engineers*.

Molenaar, M., Hill, D., and Koelman, V. 2011. *Downhole Tests Show Benefits of Distributed Acoustic Sensing Oil Gas J.* **109** (1): 82–85.

Miller, C. et al.: "Evaluation of Production Log Data from Horizontal Wells Drilled in Organic Shales" paper SPE 144326 presented at North American Unconventional Gas Conference and Exhibition, 2011.

McGinley, M., Zhu, D., Hill, A.D 2015. The effects of fracture orientation and anisotropy on hydraulic fracture conductivity in the Marcellus Shale. Presented at the SPE Annual Technical Conference and Exhibition, Houston, Texas, USA, 28–30 September 2015. SPE-174870-MS.

Suarez-Rivera, R., Deenadayalu, C., Gathogo, P., Chertov, M. and Kunjir, R. 2011. Improving Horizontal Completions on Heterogeneous Tight Shales. Paper CSUG/SPE 146998 presented at the Canadian Unconventional Resources Conference, Calgary, Alberta, Canada, 15- 17 November.

Serajian, V. and Ghassemi, A. 2011. Hydraulic Fracture Initiation from a Wellbore in Transversely Isotropic Rock. Paper ARMA 11-201 presented at the 45th U Rock Mechanics/Geomechanics symposium, San Francisco, Califrnia,usa, 26-29- june.

Spain, D.R., I. Gil, H. Sebastian, P.S. Smith, J. Wampler, S. Cadwallader, M. Graff. 2015. Geo-Engineered completion optimization: an integrated, multidisciplinary approach to improve stimulation efficiency in unconventional shale reservoirs. SPE 172921. Presented at the SPE Middle East Unconventional resources conference and exhibition held in Muscat, Oman, 26-28 January.

Shi, J-Q. and Durucan, S., 2016. Near-exponential relationship between effective stress and permeability of porous rocks revealed in Gangi's phenomenological models and application to gas shales, *International Journal of Coal Geology* **154–155**, 111–122.

Slocombe, R., A. Acock, K. Fisher, A. Viswanathan, C. Chadwick, R. Reischman, and E. Wigger, 2013, Eagle Ford completion optimization using horizontal log data: Presented at the Annual Technical Conference and Exhibition. New Orleans, Louisiana, USA 30 September-2 October, 2013SPE-166242-MS.

Stegent, N. A., Wagner, A. L., Mullen, J. and Borstmayer, R. E. 2010. Engineering a Successful Fracture-Simulation Treatment in the Eagle Ford Shale. presented at the SPE Tight Gas Completion Conference held in San Antonio, Texas, USA, 2–3 November. SPE-136183-MS

Paronish, Thomas J., Shuvajit Bhattacharya, and Timothy Carr. Integrated Geologic Analysis from Two Marcellus Shale Science Wells in Northeastern West Virginia. Poster presentation given at AAPG 2016 Annual Convention and Exhibition, Calgary, Alberta, Canada, June 19-22, 2016.

Ugueto, G. A., R.T. Huckabee, M.M. Molenaar, et al. 2016. Perforation cluster efficiency of cemented plug and perf limited entry completions: insights from fiber optics diagonstics. SPE-179124-MS. Presented at the SPE Hydraulic Fracturing Technology Conference held in The Woodlands, Texas, 9-11 February.

Wutherich, K. D., and Walker, K. J., 2012. Designing Completions in Horizontal Shale Gas Wells – Perforation Strategies. Paper SPE 155485 presented at the Americas Unconventional Resources Conference, Pittsburgh, Pennsylvania, 5–7 June.

Waters G., H. J. 2006. Use of Horizontal Well Image Tools To Optimize Barnett Shale Reservoir Exploitation. Paper SPE 103202. Presented at the SPE Annual Technical Conference and Exhibition, San Antonio, Texas, September 24-27.

Walsh, J.B. 1981. Effect of pore pressure and confining pressure on fracture permeability. *International Journal of Rock Mechanics and Mining Sciences& Geomechanics Abstracts* **18** (5): 429–435.

Zamirian. M, 2015. *New Experimental Approach to Measure Petrophysical Properties of Organic-Rich Shales*. Ph.D. Dissertation, West Virginia University, Morgantown, WV (2015).